

Correlated Random Walks in Dynamically Disordered Systems

R. Hilfer and R. Orbach

Department of Physics and Solid State Science Center
University of California, Los Angeles, CA 90024, USA

in: Dynamical Processes in Condensed Molecular Systems,
J. Klafter et al. World Scientific, Singapore, 1989, p.175-202

Abstract

We discuss correlated hopping motion in a dynamically disordered environment. Particles of type A with hopping rate $1/\tau_A$ diffuse in a background of B-particles with hopping rate $1/\tau_B$. Double occupancy of sites is forbidden. Without correlations the limit $\tau_B/\tau_A \rightarrow \infty$ corresponds to diffusion on a percolating network, while the case $\tau_B = \tau_A$ is that of self-diffusion in a lattice gas. We consider also the effect of correlations. In general these will change the transition rate of the A-particle to the previously occupied site as compared to the rate for transitions to all other neighbouring sites. We calculate the frequency dependent conductivity for this model with arbitrary ratio of hopping rates and correlation strength. Results are reported for the two dimensional hexagonal lattice and the three dimensional face centered cubic lattice. We obtain our results from a generalization of the effective medium approximation for frozen percolating networks. We predict the appearance of new features in real and imaginary part of the conductivity as a result of correlations. Crossover behaviour resulting from the combined effect of disorder and correlations leads to apparent power laws $\text{Re } \sigma(\omega) \sim \omega^y$ with $0 < y < 1$ over roughly one to two decades in frequency. In addition we find a crossover between a low frequency regime where the response is governed by the rearrangements in the geometry and a high frequency regime where the geometry appears frozen. We calculate the correlation factor for the d. c. limit and check our results against Monte Carlo simulations on the hexagonal and face centered cubic lattices for the case $\tau = 1$ and $\tau = \infty$. In all cases we find good agreement.

CONTENTS

1. Introduction	2
2. Formulation of the Model	4
2.1. Correlated Hopping in a Frozen Percolation Network	4
2.2. Correlated Hopping in a Dynamic Percolation Network	6
3. Frozen Disorder: Correlated Effective Medium	7
4. Dynamic Disorder: Renewal Approach	10
5. Results	11
6. Discussion and Conclusions	18
Acknowledgement	20
References	20

[page 176, §1]

1. Introduction

[176.1.1] A large variety of dynamic phenomena in condensed systems can be described by a lattice gas model. [176.1.2] Examples include transport in superionic solids, phase separation in binary alloys, kinetics of spin models, diffusion in metal-hydrogen systems or order-disorder phenomena in chemisorbed monolayers at surfaces [1–4]. [176.1.3] Moreover, the popular model of hopping transport on a percolating network can be viewed as a special case. [176.1.4] This is seen by considering a lattice gas with two species of particles, A and B, for the case where the B-particles are frozen into some random configuration. [176.1.5] If, as usual, the A-particles are allowed to hop only into vacant lattice sites then the problem is that of diffusion in a frozen disordered environment. [176.1.6] Our interest in this problem stems from a case in which the B-particles are not completely immobile, but very slow compared to the A-particles. [176.1.7] The general objective in this paper will be to calculate the transport coefficients for the A-particles.

[176.2.1] More specifically, we are motivated by the problem of calculating the frequency dependent conductivity of β'' -alumina, a superionic conductor, well known for its ability to transport a variety of cations [5]. [176.2.2] Na^+ /Bapp- β'' -alumina is a layered compound where Na^+ -ions hop between the sites of a hexagonal lattice forming a stack of two dimensional conduction planes [6]. [176.2.3] The activation energy for Na^+ is roughly 0.35 eV while that for Bapp is approximately 0.58 eV [5]. [176.2.4] Thus at sufficiently low temperatures the Bapp-ions are essentially frozen. [176.2.5] They play the role of the B-particles in the lattice gas described above. [176.2.6] At higher temperatures the Bapp become mobile. [176.2.7] Now the Na^+ -ions (A-particles) experience a dynamic instead of a frozen disordered environment. [176.2.8] The fundamental parameter characterizing the different time scales in the problem is the ratio $\tau = \tau_B/\tau_A$ between the characteristic hopping time τ_B of the Bapp and τ_A of the Na^+ -ions.

[176.3.1] Despite its conceptual simplicity the model contains many interesting features, even if we neglect for the moment all interactions between particles, except, of course, the hard core repulsion. [page 177, §0] [177.0.1] The hard core repulsion prevents double occupancy of lattice sites. [177.0.2] In the limit $\tau \rightarrow 1$ the tracer diffusion coefficient for the A-particle shows pronounced correlation effects [7]. [177.0.3] On the other hand in the limit $\tau \rightarrow \infty$ the system will exhibit a percolation transition [8]. [177.0.4] For low concentrations of B-particles the A-particles can diffuse along an infinite network of vacancies while at

high concentrations they are confined to finite clusters, and there will be no long range transport.

[177.1.1] Generally the system discussed above can be described by a many particle master equation [1]. [177.1.2] This remains true even if interactions between particles are included. [177.1.3] In the case of $\text{Na}^+/\text{Bapp-}\beta''$ alumina the Coulomb repulsion between the mobile ions will be important. [177.1.4] Additional correlations can arise from lattice relaxation effects, or from simultaneous hops of groups of ions. [177.1.5] The latter is a well known phenomenon for the related β -alumina. [177.1.6] Clearly the problem has to be simplified even if one resorts to a computer simulation. [177.1.7] A careful Monte-Carlo-study of the tracer diffusion problem was carried out by Kehr, Kutner and Binder [7, 9–12]. [177.1.8] They focussed on the case $\tau = 1$ on a face centered cubic (fcc) lattice, and considered systems with and without short range attractive/repulsive interactions. [177.1.9] Theoretical attempts [13–15] have also concentrated on the case $\tau = 1$ and were therefore unable to reproduce the percolation transition for $\tau \rightarrow \infty$. [177.1.10] In this paper we present a theory for general τ which allows to incorporate correlation effects arising from the blocker dynamics or from other sources such as particle interactions.

[177.2.1] Let us first discuss the general framework of our approach. [177.2.2] Instead of focussing on the case $\tau = 1$ the basic idea is to start from the frozen problem, i. e. $\tau = \infty$. [177.2.3] We discuss the diffusion of a single A-particle in the percolation geometry produced by the immobile B-particles. [177.2.4] Interactions between the particles lead to correlations for the random walk of the A-particle. [177.2.5] In general the effect of such correlations is to change the transition probabilities to nearest neighbours of the particle [16]. [177.2.6] In particular let us assume that the primary effect is to change the transition rate to the site that was occupied before the last step. [177.2.7] Thus we assume that the A-particle has a memory of its previous position, and consequently its random walk no longer has the Markov property. [177.2.8] The corresponding problem on a regular lattice is well known [17–20] and can be solved exactly. [page 178, §0] [178.0.1] This allows us to formulate a generalized effective medium theory for the correlated hopping of an A-particle on the frozen disordered network.

[178.1.1] Finally the B-particles are allowed to move, i. e. $\tau < \infty$, and the A-particle now experiences a dynamic disordered environment. [178.1.2] The solution to this dynamic percolation problem can be expressed in terms of the solution for the frozen problem. [178.1.3] The result is valid for arbitrary τ and allows to incorporate correlation effects via the special transition rate for transitions to the previously occupied site. [178.1.4] The main advantage of this approach is its simplicity. [178.1.5] The three main parameters are the concentration of B-particles, p , the ratio of attempt frequencies, τ , and the ratio between the hopping rates for return to previously occupied sites and transitions to other neighbours, b . [178.1.6] The first two are essentially fixed from the experiment, while b can be determined from a measurement of the conductivity at any single frequency, e. g. at $\omega = 0$.

[178.2.1] The objective of this paper, as mentioned in the beginning, is the calculation of the frequency dependent conductivity for the A-particles. [178.2.2] In addition we wish to evaluate the correlation factor for the selfdiffusion constant in the d. c. limit. [178.2.3] We assume here that the B-particles do not contribute to the conductivity. [178.2.4] We will

present results for the hexagonal and the fcc-lattice. [178.2.5] The first because of its low coordination number and its relevance for $\text{Na}^+/\text{Bapp-}\beta''\text{-alumina}$. [178.2.6] The second because of the possibility to compare with d.c. results from extensive Monte-Carlo simulations in the literature.

[178.3.1] For the a.c. response we find a crossover between a low frequency regime dominated by the effects of blocker motion, and at high frequency regime in which the blockers, or equivalently vacancies, appear to form a frozen network. [178.3.2] In addition we predict the appearance of novel features in the real and imaginary part as a result of correlations. [178.3.3] In the d.c. limit we calculate the correlation factor for the self diffusion coefficient. [178.3.4] It interpolates smoothly between the case $\tau = 0$ and $\tau \rightarrow \infty$. [178.3.5] Although our theory does not contain adjustable parameters for the uncorrelated case ($b = 1$) we find good agreement with Monte-Carlo simulations by Kehr, Kutner and Binder [10, 11]. Our results will be presented in Section 5 and are then discussed in Section 6. [page 179, §0] [179.0.1] In the next section we formulate our model. [179.0.2] In Section 3 we treat the correlated random walk in a frozen disordered environment, and in Section 4 we use the result from Section 3 as input for the dynamic problem.

2. Formulation of the Model

2.1. Correlated Hopping in a Frozen Percolation Network

[179.1.1] Consider the random walk of a single particle of type A in a percolating network on a regular lattice. [179.1.2] We will always take the lattice constant of the underlying lattice to be unity. [179.1.3] For simplicity we consider the case of bond percolation instead of site percolation. [179.1.4] That is, the bonds of the regular lattice are assumed to be blocked by B-particles (blockers) with probability p . [179.1.5] If a bond is blocked by a B-particle it cannot be crossed by the A-particle (walker). [179.1.6] We assume that the walker has a memory of its previous step. [179.1.7] It returns with a transition rate ω_b , to the previously visited site, and jumps with a rate ω to any other of the nearest neighbour sites. [179.1.8] The ratio $b = \omega_b/\omega$ is a measure of the strength of the memory correlations. [179.1.9] For $b > 1$ the walker returns preferentially to its previously visited site, and we will refer to this case as “enhanced reversals”. [179.1.10] In the case $b < 1$ the walker tends to avoid the previously visited site and this will be termed “reduced reversals”. [179.1.11] As usual, we are interested in the autocorrelation function $P(i, t) = P(\vec{r}_i, t | r_0, 0)$, i.e. the probability density to find the walker at site i at time t if it started from site 0 at time 0. [179.1.12] We will show below that the problem can be formulated as a system of second order equations for the $P(i, t)$ which reads

$$\begin{aligned} & \frac{d^2}{dt^2} P(i, t) + (\gamma_i + \omega_b - \omega) \frac{d}{dt} P(i, t) \\ & = \omega \sum_{j \{i\}} A_{ij} \frac{d}{dt} [P(j, t) - P(i, t)] + \omega \gamma_i \sum_{j \{i\}} A_{ij} [P(j, t) - P(i, t)] \end{aligned} \quad (2.1a)$$

where $\gamma_i = \omega_b + \omega(z_i - 1)$ and z_i is the coordination number of site i . [179.1.13] The symmetric quantities $A_{ij} = A_{ji}$ represent the bond disorder and are defined as

$$A_{ij} = \begin{cases} 1 & \text{if the bond } [ij] \text{ is vacant,} \\ 0 & \text{if the bond } [ij] \text{ is blocked.} \end{cases} \quad (2.1b)$$

[page 180, §0] [180.0.1] The summation in eq. (2.1a) runs over the nearest neighbour sites j of site i . [180.0.2] Note that in the uncorrelated case, $b = 1$, eq. (2.1) reduces to the usual master equation for a random walk on a bond percolation network if one replaces $P(i, t)$ by the sum of P and its derivative.

[180.1.1] Equation (2.1) has to be supplemented by initial conditions for $P(i, t)$ and its derivative. [180.1.2] Special attention has to be paid to the condition on $\frac{d}{dt}P(i, t)$ and its derivative. [180.1.3] The correct choice is

$$P(i, 0+) = \delta_{i0} \quad (2.2a)$$

$$\begin{aligned} \frac{d}{dt}P(i, 0+) &= [\omega_b + \omega(z_i - 1)] \frac{1}{z_i} \sum_{j \in \{i\}} A_{ij} [P(j, 0+) - P(i, 0+)] \\ &= \gamma_i / z_i \sum_{j \in \{i\}} A_{ij} (\delta_{j0} - \delta_{i0}) \end{aligned} \quad (2.2b)$$

where the symbol $0+$ stands for the limit $t \rightarrow 0$ from above. [180.1.4] Note that γ_i / z_i is the average transition rate out of the starting point.

[180.2.1] We now derive eq. (2.1) as the equations of motion for our correlated random walk. [180.2.2] This will be done by a suitable reformulation of the equations for the correlated random walk on the regular lattice [19], and subsequent generalization to the disordered case. [180.2.3] Consider therefore the random walker on a regular lattice. [180.2.4] The random walker has a memory of its previous step and as a consequence its walk is not markovian, i. e. the transition probabilities are not completely determined by the currently occupied site. [180.2.5] However a markovian description can be obtained by introducing an enlarged state space with internal states which correspond to the previously occupied sites [21]. [180.2.6] Therefore the central quantity is the probability density $P(i, j, t)$ to find the walker at site i at time t given that it arrived at i via a direct transition from site j . [180.2.7] Thus j labels the previously occupied site or history. [page 181, §0] [181.0.1] Then the symmetric probability density $P(i, t)$ is obtained from $P(i, j, t)$ by a summation over all possible histories

$$P(i, t) = \sum_{j \in \{i\}} P(i, j, t) \quad (2.3)$$

where the sum runs over all nearest neighbour sites j of site i . [181.0.2] The conditional probability densities $P(i, j, t)$ obey the master equation

$$\frac{d}{dt}P(i, j, t) = \omega_b [P(j, i, t) - P(i, j, t)] + \omega \sum_{k \neq i} [P(j, k, t) - P(i, j, t)] \quad (2.4)$$

where the sum runs over all nearest neighbours k of site j except for site i on the regular lattice. [181.0.3] This is the starting point for deriving eq. (2.1).

[181.1.1] Equation (2.4) can now be reformulated by first writing it in a more symmetric form. [181.1.2] Using eq. (2.3) we can rewrite eq. (2.4) as

$$\frac{d}{dt}P(i, j, t) = (\omega_b - \omega)P(j, i, t) + \omega P(j, t) - \gamma P(i, j, t) \quad (2.5)$$

where $\gamma = \omega_b + (z - 1)\omega$, and z denotes the coordination number of the lattice. [181.1.3] Note that eq. (2.5) reduces to the master equation for a random walk on a regular lattice if one sets $b = 1$ and sums over all sites j which are nearest neighbours of site i . [181.1.4] Next we

differentiate eq. (2.5) and sum over j . [181.1.5] We then employ it for i and j interchanged to eliminate the term $\frac{d}{dt}P(j, i, t)$ and find

$$\begin{aligned} & \frac{d^2}{dt^2}P(i, t) + \gamma \frac{d}{dt}P(i, t) \\ &= (\omega_b - \omega)\gamma P(i, t) + \omega \sum_{j\{i\}} \frac{d}{dt}P(j, t) - (\omega_b - \omega)\gamma \sum_{j\{i\}} P(j, i, t). \end{aligned} \quad (2.6)$$

[181.1.6] Solving eq. (2.5) for $P(j, i, t)$ and inserting the result into eq. (2.6) one obtains a closed second order equation for $P(i, t)$

$$\begin{aligned} & \frac{d^2}{dt^2}P(i, t) + (\gamma + \omega_b - \omega) \frac{d}{dt}P(i, t) \\ &= \omega \sum_{j\{i\}} \frac{d}{dt}[P(j, t) - P(i, t)] + \omega\gamma \sum_{j\{i\}} [P(j, t) - P(i, t)] \end{aligned} \quad (2.7)$$

where the summations, as before, run over all nearest neighbour sites j of site i . [page 182, §0] [182.0.1] Eq. (2.7) contains the same information as eq. (2.4) but no longer involves the directional quantities $P(i, j, t)$. [182.0.2] This form can now be used to introduce disorder and it leads directly to eq. (2.1). [182.0.3] We now turn to the introduction of a time dependent network.

2.2. Correlated Hopping in a Dynamic Percolation Network

[182.1.1] Consider a system where the configuration of accessible sites fluctuates in time. [182.1.2] We are interested in the case where the B-particles perform a random walk. [182.1.3] Because we are dealing with bond percolation this random walk occurs on the dual lattice. [182.1.4] In an elementary step a blocking bond swings around either one of its end points through an angle $\pm 2\pi/z$ where z is the coordination number of the underlying lattice. [182.1.5] It then occupies the new bond position if it is vacant. [182.1.6] This process is repeated on the average after a time τ_B which is the characteristic time scale for the blocker motion. [182.1.7] In Figure 2 we depict the possible rotations of a B-particle for the case of a hexagonal lattice. [182.1.8] This model has been termed “dynamic bond percolation” model [22]. [182.1.9] The characteristic hopping time for a single B-particle is called τ_B . [182.1.10] The ratio $\tau = \tau_B/\tau_A$ between the typical hopping time of the blockers and the walker will be the main variable characterizing the dynamics of the environment.

[182.2.1] Equation (2.1) must be generalized to allow for time dependent transition rates. [182.2.2] Therefore we have to consider an equation of the form

$$\begin{aligned} & \frac{d^2}{dt^2}P(i, t) + (\gamma_i + \omega_b - \omega) \frac{d}{dt}P(i, t) \\ &= \omega \sum_{j\{i\}} A_{ij}(t) \frac{d}{dt}[P(j, t) - P(i, t)] + \omega\gamma_i \sum_{j\{i\}} A_{ij}(t) [P(j, t) - P(i, t)] \end{aligned} \quad (2.8a)$$

where now the coefficients A are time dependent,

$$A_{ij}(t) = \begin{cases} 1 & \text{if the bond } [ij] \text{ is vacant at time } t, \\ 0 & \text{if the bond is occupied by a blocker at time } t. \end{cases} \quad (2.8b)$$

[page 183, §0] [183.0.1] The time dependence of these coefficients could in principle be determined from the many particle master equation for all blockers. [183.0.2] However, because that equation is much too complicated we will approximate the true time dependence by

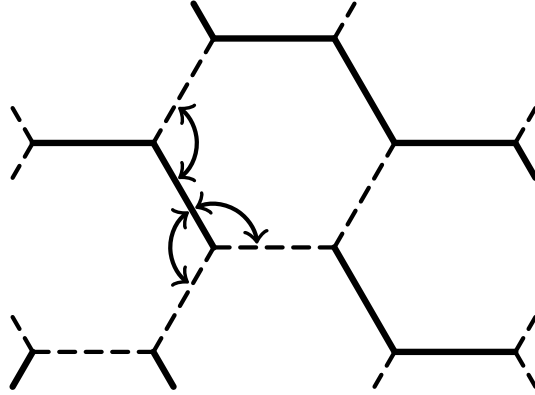


FIGURE 1. Blocker motion on the hexagonal lattice. Three possible elementary rotations of a blocking bond around either one of its endpoints are indicated by arrows. Full lines represent blocked bonds, dashed lines represent open bonds.

a simple renewal model in Section 4. [183.0.3] Equation (2.8) completes the formulation of the model. [183.0.4] We remark here that other forms of a two step memory are possible and may be useful for applications. [183.0.5] For example one can consider enhanced or reduced transitions continuing in the same direction as the last step. [183.0.6] Such correlations lead to more complicated equations, but they can be treated by the same general approach presented here.

[183.1.1] We conclude this section with the formulas that will be used to calculate the frequency dependent conductivity $\sigma(\omega)$ from $P(i, t)$. [183.1.2] This is done via a generalized Einstein relation which reads

$$\sigma(\omega) = \frac{\rho e^2}{k_B T} D(\omega) \quad (2.9a)$$

where ρ is the carrier density, e their electric charge, k_B , the Boltzmann constant, T the absolute temperature, and $D(\omega)$ the generalized frequency dependent diffusion coefficient. [page 184, §0] [184.0.1] $D(\omega)$ will be calculated in standard fashion from [23]

$$D(\omega) = -\frac{\omega^2}{z} \int_0^\infty \sum_{\vec{r}_i, \vec{r}_0} (\vec{r}_i - \vec{r}_0)^2 e^{-i\omega t} P(\vec{r}_i, t | \vec{r}_0, 0) dt \quad (2.9b)$$

where $P(\vec{r}_i, t | \vec{r}_0, 0)$ is the solution to eq. (2.8) or eq. (2.1) for the frozen case. [184.0.2] The latter will be determined in the next section.

3. Frozen Disorder: Correlated Effective Medium

[184.1.1] In this section we develop an effective medium approximation to solve eq. (2.1) with initial conditions (2.2) describing the correlated random walk of an A-particle in the frozen background of blockers. [184.1.2] This is possible because the correlated walk on the regular lattice can again be solved exactly. [184.1.3] We will derive a selfconsistent equation similar to that for the generalized diffusion coefficient in the well known effective medium treatment of random walks on a frozen percolating network [24–28]. [184.1.4] In our case, however, the solution of the selfconsistent equation is only an intermediate step from which the generalized diffusion coefficient has to be calculated [29].

[184.2.1] We start by Laplace transforming eq. (2.1) and inserting the initial conditions.
 [184.2.2] This gives

$$\begin{aligned} & u(u + \gamma_i + \omega_b - \omega)P_i(u) - (u + \gamma_i + \omega_b - \omega)\delta_{i0} - (\omega_b - \omega)\frac{1}{z_i}\sum_{j\{i\}}A_{ij}(\delta_{j0} - \delta_{i0}) \\ &= \omega(u + \gamma_i)\sum_{j\{i\}}A_{ij}[P_j(u) - P_i(u)] \end{aligned} \quad (3.1)$$

where we have written $P_i(u) = P(i, u) = \int_0^\infty e^{-ut}P(i, t)dt$ to shorten the notation. [184.2.3]
 For a selfconsistent treatment of the disorder we have to compare eq. (3.1) with the same equation for the regular reference lattice where we allow the kernel $A^0(u)$ to be frequency dependent. [page 185, §0] [185.0.1] The equation for the regular reference lattice then reads

$$\begin{aligned} & u(u + \gamma_i + \omega_b - \omega)P_i^0(u) - (u + \gamma_i + \omega_b - \omega)\delta_{i0} - (\omega_b - \omega)\frac{1}{z_i}\sum_{j\{i\}}A^0(u)(\delta_{j0} - \delta_{i0}) \\ &= \omega(u + \gamma_i)\sum_{j\{i\}}A^0(u)[P_j^0(u) - P_i^0(u)]. \end{aligned} \quad (3.2)$$

[185.0.2] We subtract eq. (3.2) from eq. (3.1) and insert a term $A^0[P_j(u) - P_i(u)]$. [185.0.3] This gives us

$$\begin{aligned} & \left[\frac{u}{\omega A^0} \left(1 + \frac{\omega_b - \omega}{u + \gamma_i} \right) + z_i \right] (P_i - P_i^0) - \sum_{j\{i\}} (P_j - P_j^0) - \frac{\omega_b - \omega}{u + \gamma_i} \frac{1}{\omega z_i} \sum_{j\{i\}} \Delta_{ij} (\delta_{j0} - \delta_{i0}) \\ &= \sum_{j\{i\}} \Delta_{ij} (P_j - P_i) \end{aligned} \quad (3.3)$$

where we have introduced $\Delta_{ij} = (A_{ij} - A^0)/A^0$ and suppressed the dependence on u to further shorten the notation. [185.0.4] We now define the lattice Greens function associated with the reference lattice by

$$\left[\frac{u}{\omega A^0} \left(1 + \frac{\omega_b - \omega}{u + \gamma_i} \right) + z_i \right] G_{ik} - \sum_{j\{i\}} G_{jk} = -\delta_{ik}. \quad (3.4)$$

[185.0.5] Multiplication of eq. (3.3) by G_{ik} , summation over i , and use of eq. (3.4) allows us to rewrite eq. (3.3) as

$$(P_k - P_k^0) + \sum_{i,j} G_{ik} \frac{\omega_b - \omega}{u + \gamma_i} \frac{1}{\omega z_i} \Delta_{ij} (\delta_{j0} - \delta_{i0}) = - \sum_{i,j} G_{ik} \Delta_{ij} (P_j - P_i). \quad (3.5)$$

[185.1.1] As we are dealing with bond percolation it is convenient to switch from site related quantities to bond related ones. [185.1.2] This is done by writing eq. (3.5) for a second site l , and then forming the differences $Q_{kl} = P_k - P_l = -Q_{lk}$. [185.1.3] In terms of the quantities Q_{kl} one now has

$$\begin{aligned} Q_{kl} &= Q_{kl}^0 + \sum_{[ij]} (G_{ik} - G_{il} - G_{jk} + G_{jl}) \Delta_{ij} Q_{ij} \\ &\quad - \frac{1}{2} \sum_{i,j} \left[(G_{ik} - G_{il}) \frac{\omega_b - \omega}{u + \gamma_i} \frac{1}{\omega z_i} - (G_{jk} - G_{jl}) \frac{\omega_b - \omega}{u + \gamma_j} \frac{1}{\omega z_j} \right] \Delta_{ij} (\delta_{j0} - \delta_{i0}) \end{aligned} \quad (3.6)$$

where the summations run over all bonds $[ij]$. [page 186, §0] [186.0.1] As usual [24–28] one allows only a finite number of bonds (here only one bond) to fluctuate while all other bonds are given their effective medium value. [186.0.2] In this 1-bond-approximation the bond

[kl] can be chosen arbitrarily, and we choose it such that it does not touch the starting point of the random walk, i. e. $k \neq 0, l \neq 0$. [186.0.3] Then eq. (3.6) is easily solved to give

$$Q_{kl} = \frac{1}{1 - \Delta_{kl}(G_{kk} + G_{ll} - G_{kl} - G_{lk})} Q_{kl}^0. \quad (3.7)$$

[186.0.4] Up to this point we have not made use of the fact that the reference lattice is regular. [186.0.5] We assume now a regular lattice for the effective medium such that $z_i = z$ for all sites. [186.0.6] In this case the solution of eq. (3.4) is recognized as the Greens function for that lattice if one introduces the new spectral variable

$$\tilde{u} = \frac{u}{\omega A^0(u)} \left(1 + \frac{\omega_b - \omega}{u + \gamma} \right) \quad (3.8)$$

instead of u .

[186.1.1] The self consistent equation is obtained by demanding to choose a frequency dependent medium $A^0(u)$ such that it reproduces on average the behaviour of the original system, i. e. we demand $\langle Q_{kl} \rangle = \langle Q_{kl}^0 \rangle$ where $\langle \cdot \rangle$ denotes the average over all possible configurations of the bond $[kl]$. Using this condition in eq. (3.7) we find

$$1 = \left\langle \frac{1}{1 + \Delta_{kl} \left[\frac{2}{z} + \frac{2\tilde{u}}{z} G_{ii}(\tilde{u}) \right]} \right\rangle \quad (3.9)$$

where we have also used the symmetry of the Greens function and eq. (3.4) to express $G_{ij}(\tilde{u})$ in terms of $G_{ii}(\tilde{u})$. [186.1.2] The average in eq. (3.9) has to be taken with respect to the probability density $f(A_{kl})$ which was given in eq. (2.1) as $f(A_{kl}) = (1 - p)\delta(A_{kl} - 1) + p\delta(A_{kl})$. [186.1.3] Performing the average and introducing the notation $p_c = 2/z$ for the percolation threshold one finds from eq. (3.9) the selfconsistent equation

$$A^0(u) = \frac{1 - p - p_c - p_c \tilde{u} G(\tilde{u})}{1 - p_c - p_c \tilde{u} G(\tilde{u})}$$

with \tilde{u} given by eq. (3.8), and $G(u) = G_{ii}(u)$. [page 187, §0] [187.0.1] Partially solving for A^0 then leads to the functional equation

$$A^0(u) = \frac{1 - p - p_c - F(u, A^0)}{2(1 - p_c)} \left\{ 1 \pm \left\{ 1 - \frac{4(1 - p_c)F(u, A^0)}{[F(u, A^0) - 1 + p + p_c]^2} \right\}^{1/2} \right\} \quad (3.10a)$$

where

$$F(u, A^0) = p_c \frac{u}{\omega} \left(1 + \frac{\omega_b - \omega}{u + \gamma} \right) G \left\{ \frac{u}{\omega A^0(u)} \left(1 + \frac{\omega_b - \omega}{u + \gamma} \right) \right\} \quad (3.10b)$$

[187.0.2] This formulation has the advantage that it displays explicitly the two different branches of the solution. [187.0.3] The decision which branch to use is made by enforcing the correct limiting behaviour of σ . [187.0.4] This requires that we calculate first the generalized diffusion coefficient D . [187.0.5] For that we must solve eq. (2.7). [187.0.6] Fourier-Laplace transforming eq. (2.7) and using the initial conditions of eq. (2.1). [187.0.7] We obtain

$$P(\vec{k}, u) = \frac{\frac{1}{\omega A^0} + \frac{\omega_b - \omega}{u + \gamma} \frac{1}{\omega} \left(\frac{1}{A^0} - 1 \right) + \frac{\omega_b - \omega}{u + \gamma} \frac{1}{\omega} p(\vec{k})}{\frac{u}{\omega A^0} \left(1 + \frac{\omega_b - \omega}{u + \gamma} \right) + z - zp(\vec{k})} \quad (3.11)$$

where $\vec{k} = (k_1, \dots, k_d)$ denotes the wave vector, and $p(\vec{k})$ is the usual characteristic function of the random walk for the lattice under consideration, e. g. $p(\vec{k}) = \frac{1}{d} \sum_{i=1}^d \cos k_i$ for the d -dimensional simple cubic lattices.

[187.1.1] Now equation (2.9) can be employed to calculate the conductivity $\sigma(\omega)$. A straightforward calculation using $p(\vec{k})|_{\vec{k}=0} = 1$ and $\nabla_{\vec{k}}p(\vec{k})|_{\vec{k}=0} = 0$ leads to the generalized diffusion coefficient [29]

$$D_0(u) = p''(0)A^0(u)\frac{\omega}{z}(b-1+z)\frac{\frac{u}{\omega}+z}{\frac{u}{\omega}+z+2b-2} \quad (3.12)$$

as a function of $u = i\omega$. [187.1.2] Here $p''(0)$ denotes $(\nabla_{\vec{k}})^2 p(\vec{k})|_{\vec{k}=0}$, and we have used the index 0 to indicate that eq. (3.12) is valid for the frozen case, i.e. $\tau = \infty$. [187.1.3] With equations (3.12) and (3.10) we have now derived the set of selfconsistent equations for the frozen diffusion coefficient $D_0(u)$. [187.1.4] It remains to specify a particular lattice, and to solve eq. (3.10) for the case of interest. [page 188, §0] [188.0.1] That will be done in Section 5 after we have discussed how to make use of these results for the dynamic disorder problem.

4. Dynamic Disorder: Renewal Approach

[188.1.1] So far we have discussed equation (2.1). [188.1.2] We now turn to equation (2.8), i.e. we consider dynamic disorder. [188.1.3] The difficulty lies not so much in solving eq. (2.8) but in specifying the stochastic coefficients $A(t)$. [188.1.4] They are determined by the random motion of all blockers. [188.1.5] Our general strategy will be to assume a simpler form for the random process $A(t)$, and then to find a solution for eq. (2.8) which makes use of the solution for the frozen case, i.e. eq. (2.1).

[188.2.1] The basic idea is to approximate the actual correlated dynamics of the environment by a simple exponential renewal process. [188.2.2] Consider a single bond. [188.2.3] It is either occupied or vacant, and switches randomly between these two states. [188.2.4] This can be modelled by a two state Markov chain as suggested by Harrison and Zwanzig [30]. [188.2.5] Let $1/\tau_r$, be the switching frequency between the two states, i.e. τ_r is an effective renewal time. [188.2.6] Then the probability to find the bond occupied by a blocker at time t is easily seen to relax as $p + p_0 \exp(-t/\tau_r)$, where p_0 , is either $1 - p$ or $-p$ depending upon whether at time 0 the bond was occupied or not. [188.2.7] Thus, in this model, the bonds flip randomly and independently between the two states. [188.2.8] Using a 1-bond effective medium approximation, as the one described above, Harrison and Zwanzig [30] have shown that for this model the generalized diffusion coefficient is given by $D_0(u + 1/\tau_r)$ where $D_0(u)$ is the diffusion coefficient for the corresponding frozen problem (e.g. eq. (3.12)). [188.2.9] The same result, to which we will refer as the substitution rule, had been obtained by Druger, Ratner and Nitzan [31] for a model in which full configurations are renewed instead of single bonds. [188.2.10] This is not surprising because in the 1-bond-approximation the behaviour for the full lattice is calculated by considering only the possible configurations of a single bond. [188.2.11] Let us therefore approximate the dynamics of the environment by an exponential renewal process for full lattice configurations with renewal density

$$\psi_r(t) = \frac{1}{\tau_r} e^{-t/\tau_r}. \quad (4.1)$$

[page 189, §0] [189.0.1] The mean renewal time τ_r is now an effective renewal time which should be proportional to τ , the ratio of jump rates between B- and A-particles, i.e.

$$\tau_r = c\tau. \quad (4.2)$$

[189.0.2] The proportionality constant c contains the effects from correlations in the blocker dynamics that are not taken into account by the renewal approach. [189.0.3] It is, however,

not an adjustable parameter. [189.0.4] It will be determined below by comparison with well known exact results for the limit $p \rightarrow 1$ ($\tau = 1, b = 1$). [189.0.5] The substitution rule can also be obtained from a simple probabilistic argument [22]. [189.0.6] Consider the inverse Laplace transform $D_0(t)$ of $D_0(u)$ which was calculated in eq. (3.12). [189.0.7] As is well known, $D_0(t)$ is the kernel of a generalized master equation [32]. [189.0.8] Therefore it can be interpreted as a generalized time dependent transition rate, i. e. transition probability per unit time. [189.0.9] It describes the frozen problem in a mean field picture and is the proper kernel to use between renewal events. [189.0.10] Because the renewal process and the random walk of the Aparticle are independent, the transition rate for the dynamic problem at time t is the product of the corresponding rate for the frozen case and the probability that there was no renewal up to time t , i. e.

$$D(t) = D_0(t) \left[1 - \int_0^t \psi_r(t') dt' \right] = D_0(t) e^{-t/\tau_r}. \quad (4.3)$$

[189.0.11] From this one recovers the substitution rule by Laplace transformation. [189.0.12] Using eq. (4.2) we get

$$D(u) = D_0 \left(u + \frac{1}{c\tau} \right) \quad (4.4)$$

as our final result.

[189.1.1] To proceed we have to specify a particular lattice of interest, and solve eq. (3.10). [189.1.2] Before doing so we comment briefly on the relation to our previous continuous time random walk approach to the same problem [22]. [page 190, §0] [190.0.1] Here, as in our previous work we have attempted to find a framework in which correlation effects resulting purely from the dynamics of the environment can be incorporated. [190.0.2] In the present paper we have attacked the problem by considering random walks with memory which has the additional advantage that other types of correlations can be considered. [190.0.3] In our previous CTRW-approach we have attempted to incorporate correlation effects into the waiting time distribution by way of crude probabilistic and physical arguments about the nature of the deblocking mechanism. [190.0.4] This was based on the fact that the effective medium waiting time distribution below p_c is not normalized. [190.0.5] Consequently the distinction between the case above p_c and below persisted, and it was necessary to utilize the substitution rule of eq. (4.3) to treat the case above p_c . [190.0.6] In addition our previous approach was limited to the case $\tau \ll 1$. [190.0.7] Its main advantage was to exhibit the theoretical possibility of a sequential deblocking mechanism resulting in a nonmonotonous waiting time density and interesting consequences for the conductivity. [190.0.8] On the other hand our present approach applies for all τ and p . [190.0.9] It allows for other sources of correlations, and gives relatively good quantitative results. [190.0.10] This will be demonstrated in the next section.

5. Results

[190.1.1] The results for $\omega = 0$ will be expressed via the so called correlation factor f . [190.1.2] It is a measure which is often used to characterize the amount by which the self diffusion coefficient of a tracer particle in a lattice gas differs from its mean field value given by the vacancy concentration. [190.1.3] All results will be presented and discussed with the conventions $\omega = 1, p''(0) = 1$, and assuming a unit lattice constant. [190.1.4] In these dimensionless units f is defined by the equation $D(0) = f(1 - p)$ or, more generally,

$$f = \frac{D(0)}{D(\infty)} \quad (5.1)$$

because for our hopping models $(1-p) = D(\infty)$. [190.1.5] In the limit $p \rightarrow 1$ exact results for the correlation factor are known for the case $\tau = 1$ (and $b = 1$) [11, 13, 14]. [page 191, §0] [191.0.1] For the hexagonal lattice one has $f = 1/3$, while $f = 0.781..$ for the fcc lattice. [191.0.2] These values will be used below to determine c in eq. (4.2).

[191.1.1] We now have to solve eq. (3.10) in conjunction with eqs. (3.12) and (4.4) for the cases of interest, the hexagonal and face centered cubic lattice. [191.1.2] The lattice Greens functions for these situations are well known and can be expressed in terms of the complete elliptic integral of the first kind

$$K(m) = \int_0^{\pi/2} (1 - m \sin^2 \phi)^{-1/2} d\phi. \quad (5.2)$$

[191.1.3] For the hexagonal lattice we have

$$G(x) = -\frac{2(3+x)}{\pi(2+x)^{3/2}(6+x)^{1/2}} K\left(\frac{16(x+3)}{(x+2)^3(x+6)}\right). \quad (5.3)$$

For the fcc lattice the Greens function is given by

$$G(x) = -\frac{1}{\pi^2}(4+x)^{-1}K(x_+)K(x_-) \quad (5.4)$$

where

$$x_{\pm}^2 = \left(4 + \frac{x}{4}\right)^{-2} \left\{ \frac{1}{16} \left[\left(4 + \frac{x}{4}\right)^{1/2} - \left(\frac{x}{4}\right)^{1/2} \right]^4 + \left[\left(4 + \frac{x}{4}\right)^{1/2} \pm \left(3 + \frac{x}{4}\right)^{1/2} \right] \right\}. \quad (5.5)$$

[191.1.4] We now solve eq. (3.10) iteratively on the computer. [191.1.5] We stop the iteration when the maximal relative error between two consecutive solutions falls below 10^{-8} . [191.1.6] The resulting $A^0(u)$ is then used to calculate $D(u)$ according to eqs. (3.12) and (4.4). [191.1.7] The results are displayed in Figures 2 through 10.

[191.2.1] First we determine the proportionality constant c in eq. (4.2). [191.2.2] This is achieved by requiring that the calculated correlation factor reproduces the known exact results for the limit $p = 1$, $\tau = 1$, $b = 1$. [191.2.3] We find $c_{\text{hcx}} \approx 1.00$ for the hexagonal lattice, and $c_{\text{fcc}} \approx 0.16$ for the fcc lattice. [191.2.4] These numbers are difficult to determine numerically, and we estimate the error to be roughly 0.03. [191.2.5] In all subsequent calculations we then use these values for c .

[page 193, §1] [193.1.1] In Figure 2 we have extracted the correlation factor from $D(0)$ and plotted it versus blocker concentration p . [193.1.2] All curves are for the uncorrelated case, i. e. $b = 1$, on the fcc lattice. [193.1.3] We give results for $\tau = 0.1, 1, 10, 100, 1000$ and $\tau = \infty$. [193.1.4] The crosses are the results of the Monte Carlo simulation for the case $\tau = 1$ taken from Ref. [7]. [193.1.5] The circles are MC-results for $\tau = \infty$ and were taken from Ref. [10]. [193.1.6] Clearly there will be a discrepancy for this case because our results are approximate and for bond percolation while the simulation is exact and for site percolation. [193.1.7] An immediate problem is the value of p_c for which the effective medium theory gives $p_c = 1/6$ while the exact value is $p_c = 0.198..$ [8]. [193.1.8] If we simply use the exact value for p_c in our calculation we obtain the dashed line displayed in Fig. 2 which is found to be in good agreement. [193.1.9] In Fig. 3 we plot f vs. p for the hexagonal lattice. [193.1.10] Here the simulations have been taken from Ref. 10. [193.1.11] Keeping in mind that there are no free parameters (remember $b = 1$) we find very good agreement for both lattices. [193.1.12] However, additional simulation data especially for τ in the range $1 < \tau < \infty$, and a more accurate determination of c are required to fully

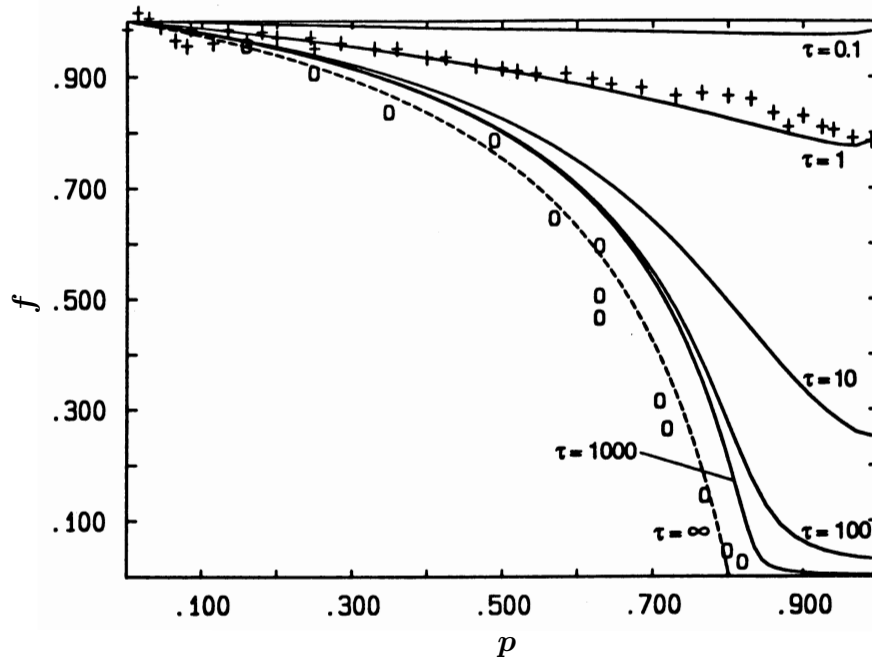


FIGURE 2. Correlation factor f as function of blocker concentration p for the face centered cubic lattice ($b = 1, c = 0.16$). The crosses are the simulation results of Ref. [7] for the case $\tau = 1$. The circles are simulation results from Ref. [10] for the case $\tau = \infty$. The dashed line is obtained by using the exact value $p_c = 0.198\dots$ from Ref. [8] instead of the effective medium value $p_c = 1/6$.

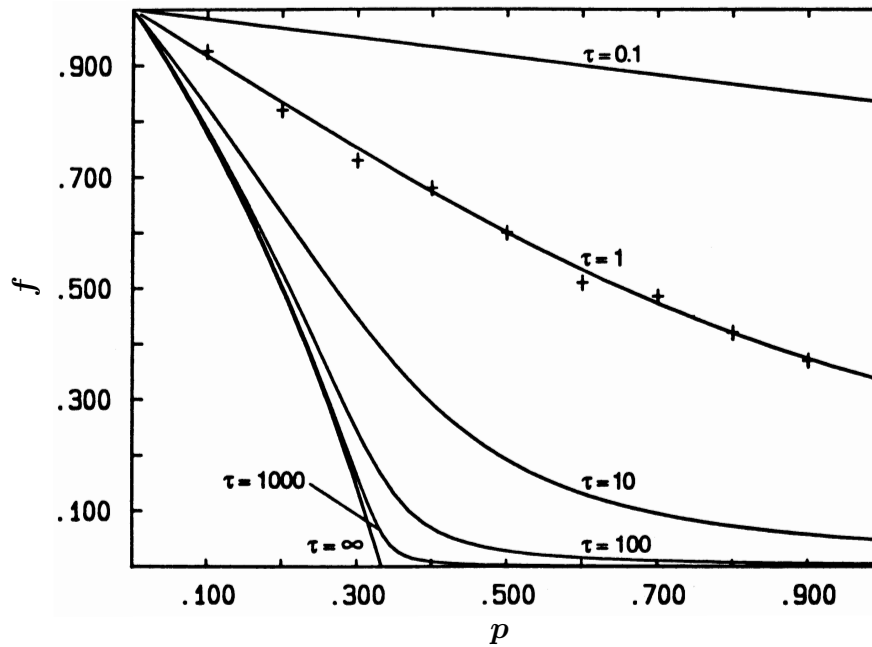


FIGURE 3. Correlation factor f vs. blocker concentration p and ratio of hopping rates τ for the hexagonal lattice ($b = 1, c = 1$). The crosses are simulation results from Ref. [12] for the case $\tau = 1$.

evaluate the quality of the theoretical results. [page 194, §0] [194.0.1] We now turn to the results for our primary objective, the frequency dependent diffusion coefficient.

[194.1.1] We consider first the uncorrelated case ($b = 1$) on the fcc-lattice. [194.1.2] In Figure 4 and Figure 5 we plot $\text{Re } D(\omega)$ over ten decades in frequency on a log-log plot. [194.1.3] Figure 4 corresponds to a blocker concentration $p = 0.9$ which is below the percolation threshold for vacancies, and shows the results for $\tau = 1, 10^3, 10^6, 10^9$ and ∞ . [194.1.4] Figure 5 has $p = 0.8$ and $\tau = 1, 10, 100, 1000, \infty$. [194.1.5] From Figure 4 we see immediately that below the percolation threshold $D(\omega)$ vanishes quadratically with frequency for $\tau = \infty$. [194.1.6] This behaviour is well known from the analysis of the EM theory for the frozen case. [194.1.7] For $\tau < \infty$ we find a crossover to a constant proportional to $1/\tau$. [194.1.8] This could have been expected because the blocker motion now allows the A-particle to get through the network although the vacancy concentration at each instant is below p_c . [194.1.9] The mobility of the A-particles will be completely determined by the mobility of the blockers. [page 197, §0] [197.0.1] The crossover frequency is seen to vary as $\omega_\tau \sim \tau^{-1/2}$. [197.0.2] This will be discussed further in the next section. [197.0.3] On the other hand above the vacancy threshold Figure 5 shows that the effect of the blocker rearrangement is only noticeable for τ values smaller than roughly 10^4 . [197.0.4] Indeed one expects that the effect of blocker motion will become negligible if $1/\tau$ is much smaller than the d. c. conductivity in the frozen case which is proportional to $1 - p - p_c$.

[197.1.1] In Figures 6 and 7 we now turn to the correlated case, i. e. $b \neq 1$. [197.1.2] Again we consider the fcc-lattice and plot the real (Fig. 6) and imaginary (Fig. 7) part of $D(\omega)$ for

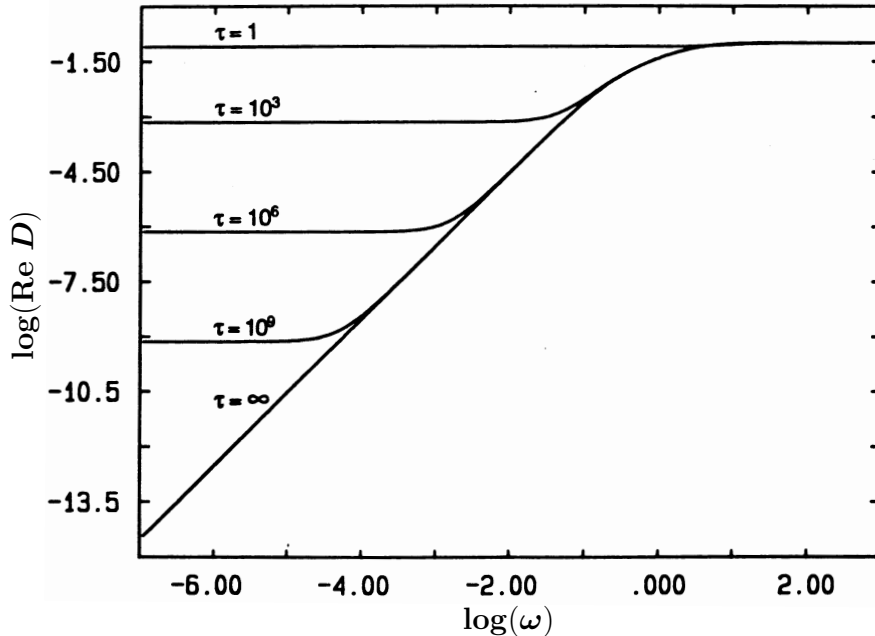


FIGURE 4. Real part of the generalized diffusion coefficient $\text{Re } D(\omega)$ for the fcc-lattice as a function of frequency ω in a logarithmic plot for several values of τ and $p = 0.9, b = 1$ ($C = 0.16$).

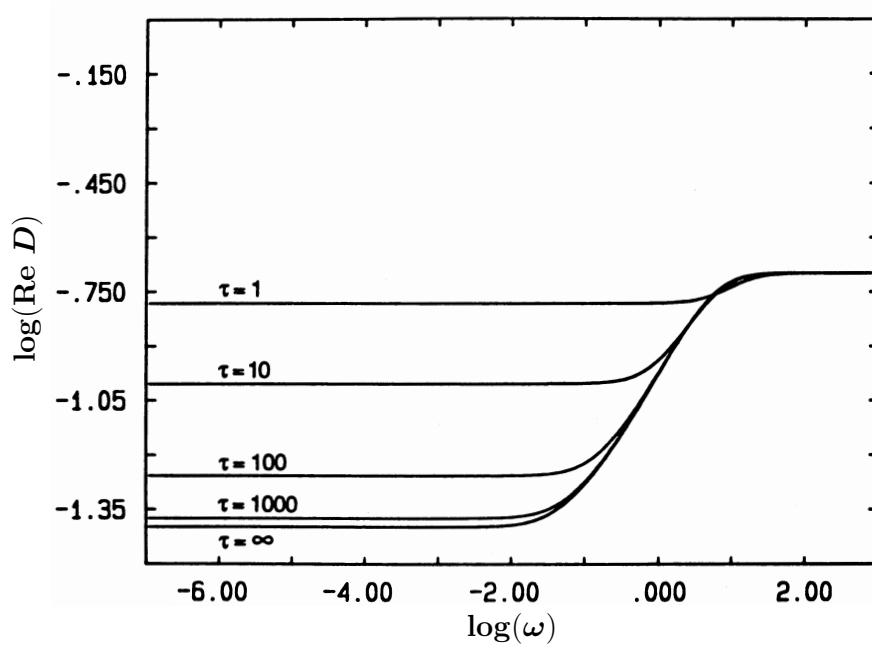


FIGURE 5. Real part of the generalized diffusion coefficient $\text{Re } D(\omega)$ for the fcc-lattice as a function of frequency ω in a logarithmic plot for several values of τ and $p = 0.8$, $b = 1$ ($c = 0.16$).

the two concentrations $p = 0.8$ and $p = 0.9$ with fixed $\tau = 100$ but variable b . [197.1.3] We have chosen $b = 0.1, 0.5, 1, 2, 10$ for the correlation factor. [197.1.4] The case $b = 1$ is included as a reference and has been distinguished graphically by a dashed line. [197.1.5] As before the real part approaches a constant as $\omega \rightarrow 0$ irrespective of p because τ is finite. [197.1.6] A new phenomenon however is the appearance of nonmonotonous behaviour for $b = 0.1$. [197.1.7] In this case $\text{Re } D(\omega)$ is found to increase at low frequencies, and to decrease at high frequencies thereby exhibiting a maximum at a finite frequency. [197.1.8] In general $\text{Re } D(\omega)$ is found to decrease as $b \rightarrow 0$ at high frequencies, and to increase at low frequencies. [197.1.9] The reverse is seen for $b \rightarrow \infty$. [197.1.10] This will also be discussed in the next section in more detail. [197.1.11] For the imaginary part of $D(\omega)$ we find a change of sign for sufficiently small $b < 1$. [197.1.12] See for example the case $p = 0.8$, $b = 0.1$. [197.1.13] On the other hand for $p = 0.9$, $b = 0.1$ there is no change of sign in the imaginary part while the real part still shows a maximum.

[197.2.1] The same calculations have been performed for the hexagonal lattice. [197.2.2] The results are displayed in Figures 8 and 9. [197.2.3] The only difference lies in the parameter values. [197.2.4] We have chosen different concentrations, $p = 0.5, 0.7$, $b = 0.1$ and fixed τ at $\tau = 10$. [197.2.5] The results show qualitatively the same behaviour as for the fcc-lattice.

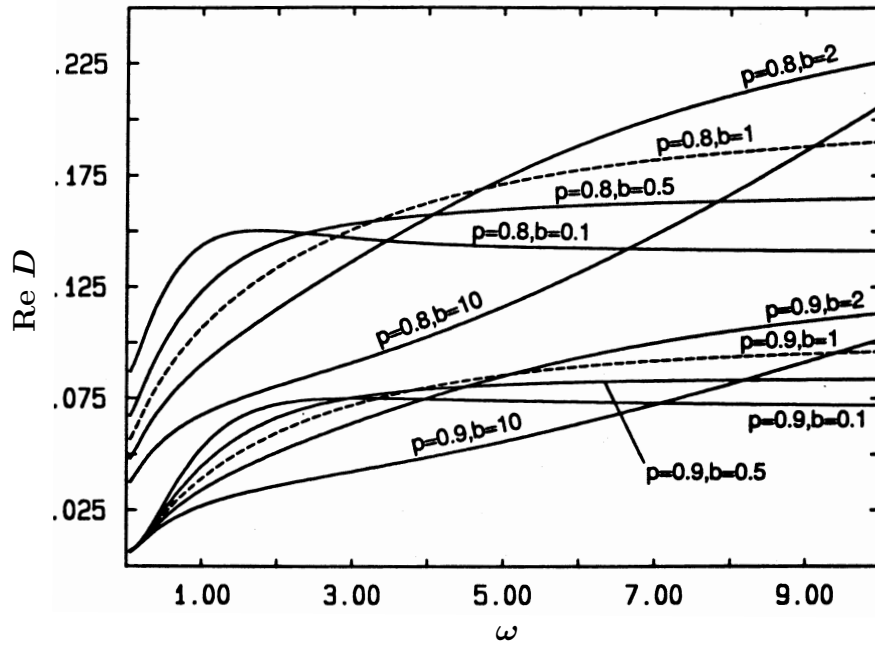


FIGURE 6. Real part of $D(\omega)$ for the fcc-lattice as a function of frequency in a linear plot for fixed $\tau = 100$, and values for b and p as indicated. The dashed line corresponds to the uncorrelated case $b = 1$.

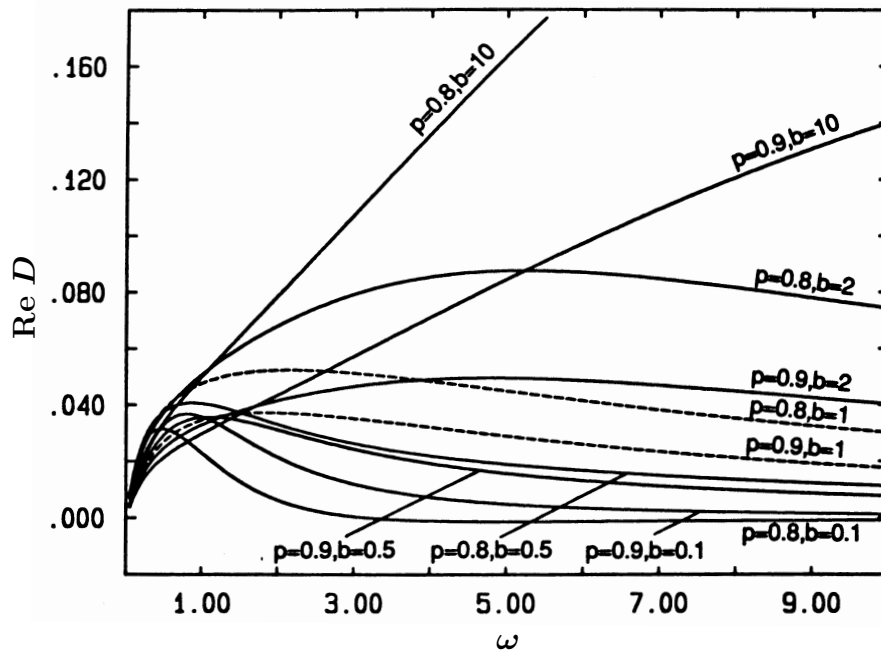


FIGURE 7. Imaginary part of $D(\omega)$ for the fcc-lattice as a function of frequency in a linear plot for fixed $\tau = 100$, and values for b and p as indicated. The dashed line is for the uncorrelated case $b = 1$.

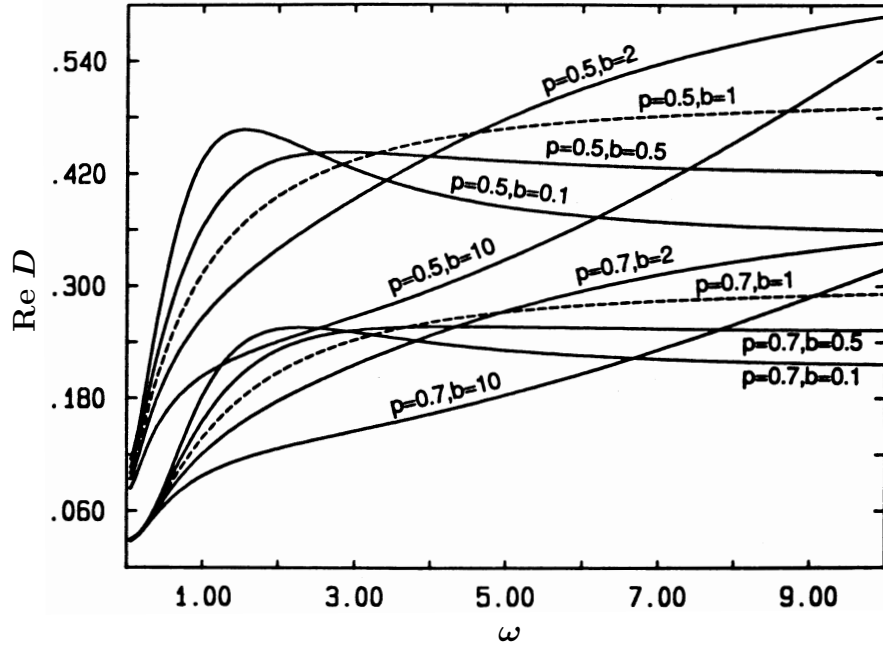


FIGURE 8. Real part of $D(\omega)$ for the hexagonal lattice as a function of frequency in a linear plot for fixed $\tau = 10$, and values for b and p as indicated. The dashed line indicates the uncorrelated case $b = 1$.

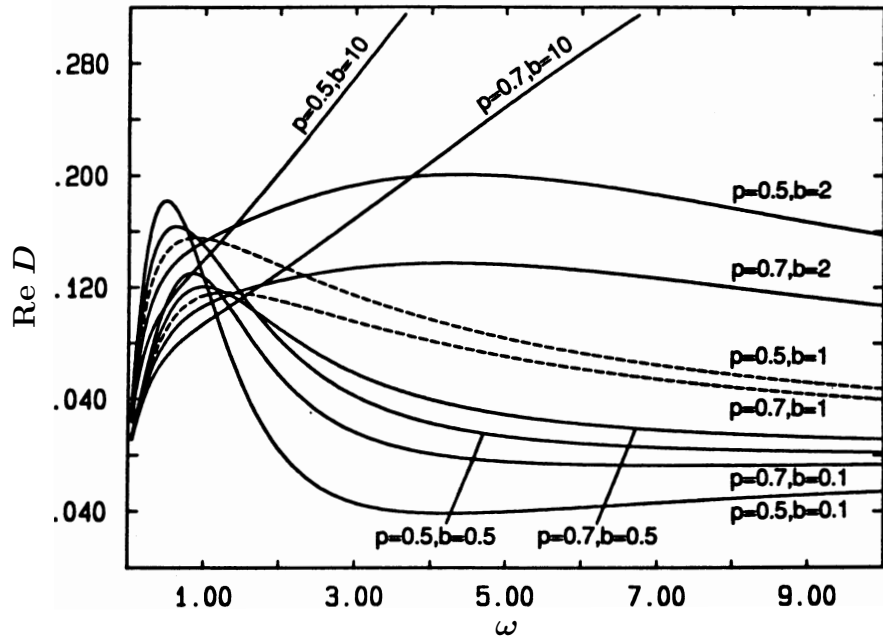


FIGURE 9. Imaginary part of $D(\omega)$ for the hexagonal lattice as a function of frequency in a linear plot for fixed $\tau = 10$, and values for b and p as indicated. The dashed line corresponds to the uncorrelated case $b = 1$.

[197.3.1] In Figure 10 we have plotted some results for the correlated case ($b \neq 1$) in a log-log plot. [197.3.2] We show $\text{Re } D(\omega)$ for $p = 0.7$, $\tau = 100$ and $b = 1, 2, 10$ on the hexagonal lattice. [197.3.3] We note that as a consequence of the correlations the crossover into the constant high frequency limit is smeared out and resembles a power law over more than a decade in frequency. [197.3.4] This is particularly apparent for the case $b = 2$.

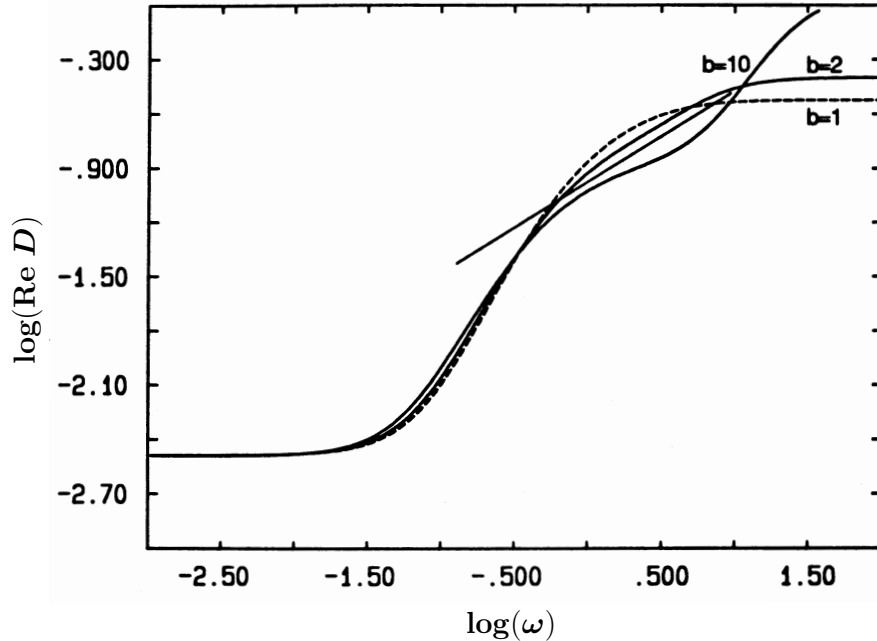


FIGURE 10. Real part of $D(\omega)$ for the hexagonal lattice plotted logarithmically against frequency for $p = 0.7$, $\tau = 100$ and $b = 1, 2, 10$. The slope of the straight line is roughly 0.5.

[page 198, §0] [198.1.1] For reference we have included a straight line into the graph whose slope is found to be roughly 0.5. [198.1.2] We remark that such a power law behaviour for the frequency dependent conductivity is often found experimentally in disordered systems. [198.1.3] As a particular example we mention Na- β -alumina where the ionic transport is also known to be highly correlated [34].

6. Discussion and Conclusions

[198.2.1] We begin with the discussion of the crossover in $\sigma(\omega)$ as a result of the mobility of the blockers. [198.2.2] As a general fact we note that the blocker motion introduces a crossover from a low frequency regime dominated by the blocker rearrangement to a high frequency regime in which the disorder appears frozen. [198.2.3] For small frequencies $\text{Re } \sigma \sim 1/\tau$ while in the high frequency regime σ behaves as for the frozen case. [198.2.4] This is independent of the correlations introduced by b .

[page 199, §1] [199.1.1] In the last section we had found from Figure 4 that the crossover frequency ω_τ between the two regimes behaves as $\omega_\tau \sim \tau^{-1/2}$. [199.1.2] This can be understood from the model of independently fluctuating bonds. [199.1.3] In this model each bond switches independently between its two states, closed and open, with a relaxation

time τ . [199.1.4] Let the system be in a stationary state at $t = 0$, i. e. when the walker starts. [199.1.5] The number of bonds that have remained in the same state since $t = 0$ decreases exponentially with time. [199.1.6] We define the crossover time as the average time after which the walker first encounters a bond that has switched at least once since $t = 0$. [199.1.7] The walker can cross a bond repeatedly as long as the bond has not switched since the start of the walk. [199.1.8] If the walker makes n steps then the average length of the time interval during which all of the it crossed bonds remain in their original state is τ/n . [199.1.9] The crossover occurs when this time equals the number of steps, i. e. when $n \cdot 1 \sim \tau/n$, where the characteristic hopping time of the walker is again assumed to be 1. [199.1.10] This immediately gives the observed $\tau^{-1/2}$ behaviour.

[199.2.1] Next we discuss the effect of correlations, i. e. the case $b \neq 1$. [199.2.2] At high frequencies the conductivity is determined mostly by the conductance (i. e. transition rate) of the last bond that was passed. [199.2.3] This conductance is increased resp. decreased per definitionem by a factor b . [199.2.4] Thus the limiting high frequency value of $\sigma(\omega)$ will be increased for enhanced reversals, $b > 1$, resp. decreased for reduced reversals, $b < 1$.

[199.3.1] At low frequencies the walker explores a much larger region, and it will begin to feel the existence of the percolation threshold. [199.3.2] Assume for the moment that the blocker conguration is frozen, i. e. $\tau = \infty$. [199.3.3] Let us consider rst the case $1 - p > p_c$, i. e. when there is an infinite network of vacancies. [199.3.4] To estimate whether the d. c. conductivity $\sigma(0)$ is enhanced or not, consider the limiting cases $b \rightarrow 1$ and $b \rightarrow \infty$ for a lattice of low coordination, e. g. the linear chain. [199.3.5] In the limit $b \rightarrow \infty$ the particle moves deterministically to the right or to the left depending upon its initial conditions. [199.3.6] For $b \rightarrow \infty$ the particle will oscillate between two sites. [199.3.7] Therefore we expect that $\sigma(0)$ will be decreased for $b > 1$, and increased for $b < 1$.

[page 200, §1] [200.1.1] A different situation arises for $1 - p > p_c$ (still with $\tau = \infty$) because now $\sigma(0) = 0$. [200.1.2] For reduced reversals ($b < 1$) the particle has a higher probability of fully exploring all the dead ends of the percolating network than for the enhanced reversals ($b > 1$). The exploration of the dead ends will however not contribute to the d. c. conductivity, and we therefore expect $\sigma(0)$ to be decreased for $b < 1$, and increased for $b > 1$.

[200.2.1] From these qualitative arguments one expects by continuity that for $1 - p > p_c$ there will be at least one point of intersection between $\text{Re } D(\omega, b = 1, \tau = \infty)$ and $\text{Re } D(\omega, b \neq 1, \tau = \infty)$. [200.2.2] For $1 - p < p_c$ there may be no point of intersection or an even number of them. [200.2.3] This is confirmed by the calculations. [200.2.4] For $1 - p < p_c$ and $\tau = \infty$ there are two points of intersection. [200.2.5] If $b < 1$ the conductivity is decreased in the very low frequency regime, increased at intermediate frequencies, and again decreased at high frequencies relative to its value for $b = 1$. [200.2.6] For small enough b a maximum can arise at a finite frequency. [200.2.7] On the other hand for $b > 1$ the conductivity is increased at very low frequencies then decreased, and finally again increased at high frequencies. [200.2.8] For the case $1 - p > p_c$ and $\tau = \infty$ we find exactly one point of intersection. [200.2.9] For $b < 1$ the conductivity is increased at low frequencies, and decreased at high frequencies as compared to its value for $b = 1$. [200.2.10] The reverse is true for $b > 1$.

[200.3.1] The maximum for $b \rightarrow 0$ arises from the competing effects of disorder induced correlations and memory induced correlations. [200.3.2] The memory correlations tend to enhance the low frequency conductivity over the values at high frequencies just as they do for the regular lattices [17–20]. [200.3.3] On the other hand the disorder has the opposite effect. [200.3.4] At high frequencies i. e. short time scales the memory correlations prevail, while at very low frequencies (i. e. on long time scales) the disorder is dominant.

If now one allows also blocker motion, i. e. for finite τ , an additional crossover arises for $1-p < p_c$. [200.4.1] At very low frequencies the diffusion is controlled by the slowly moving vacancies which can occupy every site in the underlying regular lattice, and $\sigma(0)$ will be nonzero. [200.4.2] One therefore expects that $\sigma(0)$ is increased for $b < 1$, and decreased for $b > 1$, as for a regular lattice. [page 201, §0] [201.0.1] Thus in this should be three points of intersection with the curve for $b = 1$. [201.0.2] This is indeed borne out by the numerical solution although it is a small effect as seen in Figure 10 for the case of the hexagonal lattice.

[201.1.1] In summary, in this paper we have analyzed the correlated hopping of an A-particle in a background of mobile B-particles. [201.1.2] We have calculated the corresponding frequency dependent diffusion coefficient using the substitution rule and a generalized effective medium theory for correlated diffusion. [201.1.3] We have found a rich variety of new features especially below the vacancy percolation threshold. [201.1.4] The simultaneous presence of several crossover frequencies gives rise to a complicated structure of the frequency dependent response. [201.1.5] In particular we find the possibility of a maximum in the real part at finite frequency, or apparent power law behaviour over more than a decade in frequency as a consequence of disorder and correlations. [201.1.6] Our model has a wide range of applicability. [201.1.7] As an example we refer back to the introduction and point out that our approach can be used to model the simulation results of Refs. [10] or [11] for lattice gases with short range attractive or repulsive interactions by employing the correlation parameter b . [201.1.8] Here we have applied our approach in the d. c. limit to existing Monte-Carlo simulation data of A-B-lattice gases for the uncorrelated case ($b = 1$). [201.1.9] We have found remarkably good agreement.

Acknowledgement

We gratefully acknowledge financial support from the Office of Naval Research, the National Science Foundation, and the Deutsche Forschungsgemeinschaft.

References

- [1] W. Dieterich, P. Fulde and I. Peschel, *Adv. Phys.* **29**, 527 (1980).
- [2] G.D. Mahan and F.H. Claro, *Phys. Rev. B* **19**, 1168 (1977);
- [3] D. de Fontaine in: *Solid State Physics*, H. Ehrenreich, F. Seitz and D. Turnbull (eds.), Vol **34**, Academic Press, New York 1979, p. 73
- [4] K. Binder, W. Kinzel and D.P. Landau *Surf. Sci.* **117**, 232 (1982)
- [5] G.C. Farrington and P. Dunn, *Solid State Ionics* **7**, 267 (1982)
- [6] J.P. Boilot, C. 'Collin, Ph. Colomban and R. Comes, *Phys. Rev. B* **22**, 5912 (1980)
- [7] K.W. Kehr, R. Kutner and K. Binder, *Phys. Rev. B* **23**, 4931 (1981)
- [8] D. Stauffer, *Introduction to Percolation Theory*, Taylor and Francis, London 1985
- [9] R. Kutner, K. Binder and K.W. Kehr, *Phys. Rev. B* **26**, 2967 (1982)
- [10] R. Kutner and K.W. Kehr, *Phil. Mag. A* **48**, 199 (1983)
- [11] R. Kutner, K. Binder and K.W. Kehr, *Phys. Rev. B* **28**, 1846 (1983)

- [12] R. Kutner, *J. Phys. C* **18**, 6323 (1985)
- [13] P.A. Fedders and O.F. Sankey, *Phys. Rev. B* **18**, 5938 (1978)
- [14] K. Nakazato and K. Kitahara, *Prog. Theor. Phys.* **64**, 2261 (1980)
- [15] R. Tahir-Kheli and R.J. Elliott, *Phys. Rev. B* **27**, 844 (1983)
- [16] P.M. Richards in: *Physics of Superionic Conductors*, M.P. Salomon (ed.), Springer, Berlin 1979, p. 141
- [17] J. Gillis, *Proc. Camb. Phil. Soc.* **51**, 639 (1951)
- [18] C. Domb and M.E. Fisher, *Proc. Comb. Phil. Soc.* **54**, 48 (1958)
- [19] J.W. Haus and K.W. Kehr, *Solid State Commun.* **26**, 753 (1978)
- [20] M.F. Shlesinger, *Solid State Commun.* **32**, 1207 (1979)
- [21] U. Landman, E.W. Montroll and M.F. Shlesinger, *Proc. Natl. Acad. Sciences USA*, **74**, 430 (1977)
- [22] R. Hilfer and R. Orbach, *Chem. Phys.* **128**, 275 (1988)
- [23] H. Scher and M. Lax, *Phys. Rev. B* **7**, 4491 (1973)
- [24] J.A. Blackman, *J. Phys. C* **9**, 2049 (1976)
- [25] S. Summerfield, *Solid State Commun.* **39**, 401 (1981)
- [26] I. Webman, *Phys. Rev. Lett.* **47**, 1496 (1981)
- [27] T. Odagaki and M. Lax, *Phys. Rev. B* **24**, 5284 (1981)
- [28] M. Sahimi, B.D. Hughes, L.E. Scriven and H.T. Daves, *J. Chem. Phys.* **78**, 6849 (1983)
- [29] R. Hilfer and R. Orbach, to be published
- [30] A. Harrison and R. Zwanzig, *Phys. Rev. A* **32**, 1072 (1985)
- [31] S.D. Druger, M.A. Ratner and A. Nitzan, *Phys. Rev. B* **31**, 3939 (1985)
- [32] V.M. Kenkre, E.W. Montroll and M.F. Shlesinger, *J. Stat. Phys.* **9**, 45 (1973)
- [33] M.L. Glasser and I.J. Zucker. *Proc. Natl. Acad. Sciences USA* **74**, 1800 (1977)
- [34] A.S. Barker, J.A. Ditzenberger and J.P. Remeika, *Phys. Rev. B* **14**, 4254 (1976)